

Integrated Learning and Optimization for Congestion Management and Profit Maximization in Real-Time Electricity Market

Imran Pervez, Ricardo Pinto Lima, Omar Knio

^aKing Abdullah University of Science and Technology, Thuwal, 23955, Makkah, Saudi Arabia

Abstract

We develop novel integrated learning and optimization (ILO) methodologies to solve economic dispatch (ED) and DC optimal power flow (DCOPF) problems for better economic operation. The optimization problem for ED is formulated with load being an unknown parameter while DCOPF consists of load and power transfer distribution factor (PTDF) matrix as unknown parameters. PTDF represents the incremental variations of real power on transmission lines which occur due to real power transfers between two regions. These values represent a linearized approximation of power flows over the transmission lines. We develop novel ILO formulations to solve post-hoc penalties in electricity market and line congestion problems using ED and DCOPF optimization formulations. Our proposed methodologies capture the real-time electricity market and line congestion behavior to train the regret function which eventually train unknown loads at different buses and line PTDF matrix to achieve the afore-mentioned post-hoc goals. The proposed methodology is compared to sequential learning and optimization (SLO) which train load and PTDF forecasts for accuracy rather than economic operation. Our experimentation prove the superiority of ILO in minimizing the post-hoc penalties in electricity markets and minimizing the line congestion thereby improving the economic operation with noticeable amount.

Keywords: Integrated learning and optimization (ILO), sequential learning and optimization (SLO), interior point (IP) algorithm, power transfer distribution factor (PTDF), line congestion

1. Introduction

The shift towards renewables comes with several additional challenges like system operation challenges (high rate of change of frequency (RoCoF), netload (demand - renewable generation) below base load, and violation of system ramping requirements), non-dispatchability due to high-variability, forecasting challenges due to unpredictability, and reduced revenue recovery (market price - production price) of conventional generators leading to significantly high production prices during peak or mid-peak hours. In addition to renewable-related challenges, the load demand also exhibits unpredictability issues (eg., electric vehicles (EVs) may bring additional variability/uncertainty).

The above-mentioned challenges need to be tackled for an economic and reliable operation of power systems. At the heart of economic and reliable power systems operations lies economic dispatch (ED) and DC optimal power flow (DCOPF) optimization problem formulations which generates power-dispatching decisions based on various forecasts like renewable generation, load demand, power transfer distribution factor (PTDF), etc.

The ED/DCOPF follow learning and optimization (LO) pipeline. In LO, the learning phase learns/trains unknown parameters like renewable and load forecasts in the ED/DCOPF optimization model. The ED/DCOPF optimization problem using trained forecasts is then solved to generate decisions. The LO pipeline thus directly influence ED/DCOPF decisions and needs to be designed well for economic power system opera-

tions.

One of the crucial applications of power systems is the electricity market mechanisms that decide production and consumption schedules and their pricing. The electricity market operations are largely dependent on ED/DCOPF decisions which are based on different unknowns in the ED/DCOPF formulations. Inaccuracy in the forecasts of load, renewable and other unknowns in the optimization problem leads to incorrect dispatch decisions, which may significantly impact market operations and revenues. Thus, the LO pipeline must be designed to train forecasts/unknowns in the optimization problem setting to generate optimal ED decisions.

The LO pipelines in the literature are mainly classified as sequential learning and optimization (SLO) pipeline and integrated learning and optimization (ILO) pipelines as detailed in Section 2. The commonly used pipeline for power system problems is SLO which focuses on training accurate forecasts for use in optimization problems. In this work, we develop novel ILO formulations for electricity market applications.

Electricity markets are of various types like day-ahead market (DAM), intraday market (IM), real-time market (RTM), etc. The current work mainly deals with DAM and RTM where the former involves scheduling market decisions prior to real-time operation and depends on different forecasts while the latter involves scheduling real-time market operations.

Since the DAM or other future market transactions depend on weather, load and other forecasts, actual production and consumption is likely to deviate from market-cleared schedules in

real-time resulting in a supply-demand imbalance, line congestion, etc. The deviation of actual generation and demand from baseline needs to be balanced in near to real-time or real-time to avoid user inconvenience, blackouts, etc.

MOs and ISOs use smaller time-grid market mechanisms like the intraday market (IDM) and balancing market (BM) to balance supply and demand in near to real-time and real-time. The IDM and BM mechanisms solve ED/DCOPF problems in real-time to make purchasing/selling decisions for electricity from different market traders willing to generate/consume extra to ramp up/down the total system power for total supply and demand balancing and line congestion improvement.

Deviations from nominations come at higher prices thereby reducing market participant's overall revenue. Consequently, inaccuracies in forecasts will result in reduced total revenue of market participants. The forecast models in the optimization setting needs to be trained to minimize the impact of deviations from nomination. The forecast models thus require decision focused training instead of accurate training. The decision focused training will train forecasts to produce optimization decisions favoring minimizing extra costs on market participants due to supply-demand imbalance and line congestion. The concept of decision focused training is such that two forecast models with equal errors with respect to target value, one trained for better decisions while another trained for accuracy, the optimization decisions using decisively trained forecast will pose lesser extra costs on market participants compared to the model trained for accuracy. This concept is further elaborated in Section 4.

Various supervised learning algorithms have been proposed in the literature for training forecasts in the ED/DCOPF optimization setting. In [1], the authors used a Levenberg–Marquardt back-propagation (LM-BP) neural network (NN) to improve the load prediction accuracy. This is achieved by combining the gradient descent and Quasi-Newton method to ensure faster speed, accuracy, and stability. The authors in [2] used auto-machine learning (auto-ML) for feature extraction and look-ahead window (prediction horizon) size selection for look-ahead (multi-time) load forecasting. They show that the overall forecasting accuracy can be improved by optimizing hyperparameter selection. The authors in [3] proposed a transfer learning- and temporal fusion transformer (TFT) approach to train prediction models for users and buildings with small load consumption data sets. The trained model provides significant improvement in accuracy compared to existing approaches despite less data availability.

The authors in [4] used a deep neural network with an unsupervised learning algorithm for feature extraction from the data. In [5], a deep convolutional neural network (DCNN) was proposed which uses convolutional layers and extra dense layers to generate accurate load forecasting accuracy. In [6], the authors proposed a hybrid algorithm that uses convolutional neural network (CNN) to establish the load trend learning capability and long short term memory (LSTM) to capture patterns from the time-series data. A Gaussian process (GP) based load forecasting method was proposed in [7]. The proposed GP regression model employs compositional kernels to deal with the high di-

mensional data by giving weightage to the most important input features. Training with the most important features addresses high data dimensionality and enhances the overall prediction accuracy.

The authors in [8] proposed a homogeneous ensemble-based method (random forest (RF)) for load prediction. Moreover, the authors also analyzed the importance of different features in the dataset. The overall RF algorithm outperformed other algorithms in terms of accuracy. The authors in [9] used a gradient boosting (GB) algorithm which iteratively combines several weak models (less accurate) to obtain an additive model using numerical optimization that minimizes the loss function. The proposed method was found to improve the load forecasting accuracy. The authors in [10] proposed a vector field-based support vector regression method that maps a high-dimensional feature space using a vector field to find the optimal feature space. The proposed algorithm improved the accuracy and robustness of the load prediction.

Though the above-mentioned methods improved the prediction accuracy, none of them trained the forecasts to learn better decisions.

In this work, we propose to train forecasts to learn better decisions using an integrated learning and optimization (ILO) pipeline. This, unlike SLO, offers the possibility of solving power systems problems requiring better optimization decisions rather than better forecast accuracy (eg., electricity market problems).

The literature also includes stochastic optimization techniques where supervised learning methods are used to learn forecasts in the stochastic setting of ED/DCOPF models.

The authors in [11] used stochastic model predictive control (MPC) for distributed non-linear multi-objective ED which uses data-driven scenario generation using dynamic programming (DP) by including uncertainty realizations from energy price, availability of renewable resources, and demand. Another work in [12] used stochastic MPC using data-driven scenario generation with dynamic programming (DP) for centralized ED at different time horizons including uncertainty realizations from energy price, availability of renewable resources, and demand behavior.

In [13], the authors developed centralized stochastic MPC using Monte Carlo (MC) simulation and Roulette wheel mechanism (RWM) for a contingency-constrained demand response (DR) problem by including uncertainty realizations from the availability of renewable resources, and the demand behavior. The authors in [14] developed a centralized stochastic MPC using probability distribution functions (PDFs) for multi-objective ED with several different kinds of energy sources in a networked microgrid (MG), namely by including uncertainty realizations from the availability of renewable resources. In [15], the authors proposed a centralized stochastic MPC method using the Markov chain Monte Carlo (MCMC) method for a multi-objective DR problem by including uncertainty realizations from the availability of wind resources and consumer demand.

The authors in [16] proposed centralized stochastic economic MPC for non-linear ED with balance responsible parties

(BRPs) using Monte Carlo for scenario generation by including uncertainty realizations from the availability of wind resources. The authors in [17] proposed a centralized stochastic economic hybrid with reference tracking (ERT) MPC with multi-objective ED formulation using sampling-based scenario generation by including uncertainty realizations from energy price, renewables, and demand. In [18], the authors proposed a stochastic ERT MPC for multi-objective ED using a sampling-based scenario generation approach by including uncertainty realizations from energy price and demand.

The authors in [19] proposed a centralized stochastic economic MPC for ED using Gaussian process (GP) regression for uncertainty propagation. In [20], the authors proposed a centralized stochastic economic MPC for non-linear multi-objective ED problem using scenario-based uncertainty propagation by including electricity prices, weather, and demand as uncertain variables.

The above-mentioned techniques used different stochastic MPC programming methods for various types of ED objectives. The application of stochastic MPC methods in all the above works outperformed the deterministic MPC and improved the ED optimum decision. However, the stochastic MPC and stochastic-robust MPC methods require significant computational efforts which may hamper their real-time use. Moreover, the stochastic methods are SLO-based and do not incorporate means to correct decisions so as to train the forecasts favouring better decisions.

As previously mentioned, in this work we propose to use an integrated learning and optimization (ILO) pipeline which focuses more on learning forecasts for better decisions rather than learning accurate forecasts. Moreover, the forecast after being trained is directly used for online decision-making using a deterministic setting rather than a stochastic approach which makes computationally complex online decision-making.

The application of ILO in different applications in the literature is scarce. In [26], the authors proposed a new regret function for ILO training, smart predict then optimize plus (SPO+). The authors used the SPO+ function to train the shortest path problem and compared it with SLO in terms of optimum decisions. The authors in [27] proposed an interior point (IP) algorithm-based gradient calculation for the ILO loss function and applied it to train the 0-1 knapsack problem, unit commitment, and shortest path problem. The above-mentioned works mainly used ILO to train unknown parameters in the objective function.

The authors in [28] proposed to train unknown parameters in the constraints using an IP-based gradient calculation of loss function. The authors proposed generic gradient formulations for two categories of linear programs (LPs), namely packing LP and covering LP. The authors applied their gradient formulation to train unknown parameters in the max flow transportation problem, alloy production problem, and fractional knapsack problem. In [29], the authors proposed an end-to-end wind power forecasting method to optimize the energy system by estimating wind forecasts to optimize decisions rather than wind forecasting accuracy. In [30], the authors used decision-focused learning for combinatorial optimization; however, their learn-

ing approach was based on decision rule optimization (DRO) which parametrizes both unknowns in the optimization model and the decision/policy. The decision/policy being an unknown and learned integratedly with another unknown in the optimization model may not represent the true decision/policy. The authors in [31] proposed an end-to-end approach using an energy based model to avoid calculating gradient of the regret function at each epoch and applied for load forecasting in power systems.

None of the works in the literature as per best of our knowledge formulated ILO for ED/DCOPF with multiple unknown parameters (load forecast and PTDF) in constraints. Moreover, though the work in [28] trained ILO for unknown parameters in constraints for a different application than ED, only inequality constraints were trained. The authors in [31] designed ILO formulation for forecasting the load; however, it only includes single unknown while analysing the impact of multiple equality constraints is missing. Moreover, none of the works analysed and explained the sensitivity analysis when multiple unknown parameters are included in the constraints. The application of ILO to DCOPF with multiple unknown parameters (load forecast and PTDFs) in constraints, their correlations, sensitivity analysis, their impact at different stages of market applications and ILO training formulations for multiple equality constraints in general is missing in the above-mentioned literatures.

In this work, for the first time to the best of our knowledge we develop ILO formulations to achieve economic operation in real-time market operation and non-real time generator scheduling together. The ILO formulation is designed to capture the real-time market and generator scheduling procedures to be used as a feedback for training certain unknown parameters in the equality constraints of ED/DCOPF formulations unlike SLO based open-loop training. The ILO formulation for ED is developed to obtain mainly the real-time cost-effective market operations while ILO formulation for DCOPF is developed to obtain hour-ahead and real-time cost-effective economic market operations. The training and testing results were compared with the SLO based training of ED/DCOPF unknowns and the results demonstrate a significant performance of ILO over SLO.

2. Approach

This section mainly explains the functioning of the three pipelines which clarifies the rationale for choosing ILO.

As illustrated in Fig. 1(a), the SLO pipeline has two phases, the training phase and the decision estimation phase. The training phase trains the prediction model instances ($f_{\theta}^i(A^i)$) with respect to ground truth/true parameter instances (y_i) by minimizing estimation error. The trained $f_{\theta}^i(A^i)$ is used to solve the optimization problem in the next phase making the pipeline sequential (predict and optimize sequentially).

As depicted in Fig. 1(b), the DRO pipeline trains the prediction model instances ($f_{\theta_1}^i(A^i)$) using policy approximation algorithms. The policy ($\pi_{\theta_2}^*(f_{\theta_1}^i)$) contain parameters for prediction and policy models. The corresponding regret function (L_{regret})

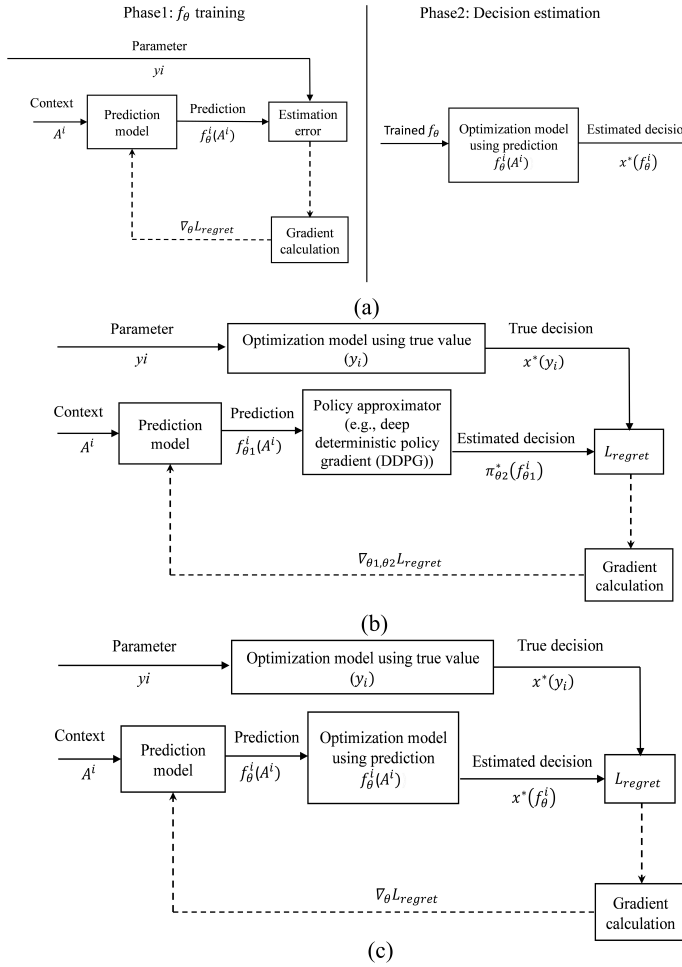


Figure 1: Comparison between different training pipelines, (a) Sequential learning and optimization (SLO), (b) decision rule optimization (DRO), and (c) Integrated learning and optimization (ILO)

is minimized to update parameters θ_1 and θ_2 corresponding to prediction model and policy model respectively.

As shown in Fig. 1(c), the ILO pipeline, the i^{th} contextual information A^i is used to evaluate the prediction $f_{\theta}^i(A^i)$. The true parameter y_i and the predicted parameter $f_{\theta}^i(A^i)$ are used to formulate the optimization problems using (3) and (4) respectively. The solution to optimization problems using $f_{\theta}^i(A^i)$ and y_i generate corresponding decisions $x^*(f_{\theta}^i(A^i))$ and $x^*(y_i)$ respectively. The decisions are used to calculate the regret function (L_{regret}) using (5). The gradient to L_{regret} is evaluated using subgradient methods like part predict then optimize plus (SPO+), interior point-based gradient, etc. The gradient of L_{regret} , $\nabla_{\theta} L_{\text{regret}}$ is used to update prediction model parameters θ .

Based on above comparisons, the SLO pipeline learns the load forecast model to minimize error concerning the ground truth load. The load forecast model trained accurately instead of being trained decision focusedly when used in optimization problem may not yield decisions favouring better power system operations despite good forecast accuracy.

The closest in decision based learning concept to ILO is the

decision rule optimization (DRO) pipeline (eg., deep reinforcement learning (DRL)) which, similar to ILO, learns the forecast model to optimize decisions. However, DRO maps the context to an approximated/parameterized decision. The DRO thus involves two approximations, forecast of optimization problem unknowns and forecast of optimization problem decisions. The parametrized DRO decisions learned integrally with other problem unknowns may not represent the true problem decisions.

3. System under Study

The current work studies the grid side operations where an independent system operator (ISO) balances supply-demand deviations from market clearing schedules in real-time by ramping-up and -down generators. The deviations from market clearing schedules are due to inaccurate load forecasts on the demand side. Moreover, real-time congestion management is done by correcting PTDF matrix coefficients to within a true PTDF range (range for which the DCOPF solution gives ED solution). The PTDF matrix represents the system topology and varies with different line and bus configurations and different system sizes. Moreover, it also represents correlations between different line impedances. The PTDF matrix therefore cannot be directly approximated using a neural network (NN) and requires transforming NN output to represent power increments and specific transmission line impedance combinations along with obeying a specific system topology which include specific line and bus configurations and different system sizes.

The grid system under study is an IEEE-14 bus system consisting of seven electricity producers/supply participants (seven generation sources) and eight consumers/demand participants (eight loads) competing in the market to supply electricity to the consumers/demand participants at MCP. ISO solves the economic dispatch (ED)/ DC optimal power flow (DCOPF) problem to supply consumer loads by scheduling different generators using load forecast. After the true load is known, the ISO corrects supply-demand imbalances and line congestion due to inaccurate load forecasts and line PTDF by solving auction balancing problem to ramp-up or -down different generators in the market at prices different than the MCP. The ISO also trades electricity with different regions if the generators within the same region cannot ramp-up/-down corresponding to load inaccuracies.

Due to price differences from MCP, the demand participants are subjected to extra payments (indirect penalty) for both over and underestimations in the load. Moreover, differences in true and forecasted PTDFs lead to higher operational costs during hour-ahead scheduling and also higher ramping costs during real-time correction. The current study thus, instead of minimizing load and PTDF forecast errors, minimizes extra payments on demand participants due to inaccurate load and PTDF forecasts using integrated learning and optimization (ILO). The ILO as explained in the upcoming sections integrates learning and optimization to capture ISO real-time correction procedures to be used as a feedback to learn the load and PTDF fore-

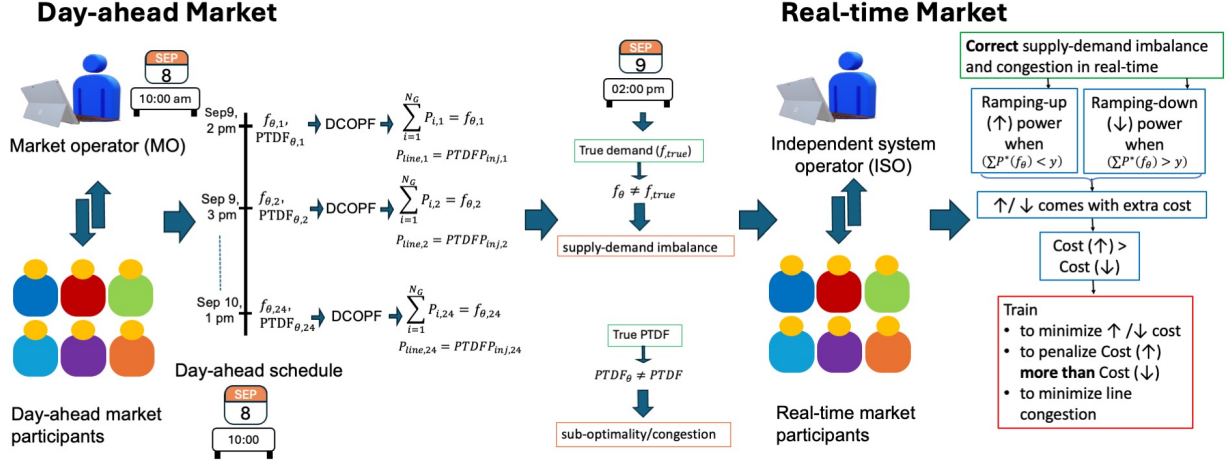


Figure 2: Two markets namely the day ahead market (DAM) and the real-time market (RTM). The market operator (MO) interacts with market participants in the DAM to schedule load and generators for next 24 hours ahead of that day (shown in Fig., say at 8 Sept. 10 am the MO schedules the loads for the next 24 hours starting from Sept. 9 pm.) The true load (f_{true}) and $PTDF$ are realized in real-time and does not matches with the predicted load and $PTDF$. The independent system operator (ISO) interacts with the market participants to correct the load and $PTDF$ in real-time. The load and $PTDF$ are trained to minimize \uparrow / \downarrow costs, penalize \uparrow more than \downarrow , and minimize congestion

casts to minimize extra payments on demand participants. The functioning of the system under study is illustrated in Fig. 2.

4. ILO Formulations for Economic Dispatch and DC Optimal Power Flow

4.1. Economic Dispatch (ED) and DC Optimal Power Flow (DCOPF)

The previous subsection explains the role of ISO in scheduling generation resources to supply demand based on the market clearing results. The ISO schedules generation resources at minimum generation cost by solving economic dispatch (ED) and DC optimal power flow (DCOPF) problems.

ED is an optimization problem for optimum resource scheduling to serve consumer electric demand while meeting various system-wide constraints at minimum generation cost. The ED optimization problem can be formulated as follows:

$$\begin{aligned} \min_P \quad & \sum_{i=1}^{N_G} \sum_{t=0}^{T-1} C_i(P_{i,t}) + \sum_{t=0}^{T-1} C_{ext,t}(s_t) \\ \text{subject to} \quad & \sum_{i=1}^{N_G} P_{i,t} = f_{true,t} - s_t \end{aligned} \quad (1)$$

$$P_{i,min} \leq P_{i,t} \leq P_{i,max}, \forall i$$

where N_G denotes the number of dispatchable units, P denotes the vector of generator power set-points, $C_i(P_{i,t})$ represents the cost of power generation for a specific generation unit which can be linear or non-linear (linear in the current study) at time step t , $f_{true,t}$ represents the total load from consumers at time step t , $P_{i,min}$ and $P_{i,max}$ respectively denotes the minimum and maximum power capacity of i^{th} generation unit, s_t denotes

the amount of power supplied by the grid at time-step t , and $C_{MCP,ext,t}(s_t)$ is the penalty associated with s_t amount of power-sharing from the grid at time-step t , T is the time-period of the look-ahead window ($T=1$ and $T=24$ for two parts of case study 1).

The above explained ED optimization model does not include line capacity constraints and does not take restraining power flow into account. Thus, another model known as DC optimal power flow (DCOPF) is needed as follows,

$$\min_P \sum_{i=1}^{N_G} \sum_{t=0}^{T-1} C_i(P_{i,t}) + \sum_{t=0}^{T-1} C_{ext,t}(s_t)$$

$$\text{subject to} \quad \sum_{i=1}^{N_G} P_{i,t} = f_{true,t} - s_t$$

(2)

$$P_{line,t} = PTDF_t P_{inj,t}$$

$$P_{i,min} \leq P_{i,t} \leq P_{i,max}, \forall i$$

$$P_{line,i,min} \leq P_{line,i,t} \leq P_{line,i,max}, \forall i$$

where $P_{line,t}$ denotes the vector of line flows, $PTDF$ (power transfer distribution factor) is a matrix to map injected power P_{inj} to line flows, $P_{line,i,min}$ and $P_{line,i,max}$ respectively denotes the minimum and maximum line flows for each line, all at time step t .

4.2. Integrated Learning and Optimization

The ILO involves training a prediction model by mapping context to decisions to minimize the downstream cost. An optimization problem can be formulated as

$$x^* = \min_x C(x) \quad \text{s.t. } g(x) \quad (3)$$

where $x \in \mathfrak{X}^d$ is a decision variable in d space, $C(x)$ is the objective/cost function, and $g(x)$ represent the set of constraints. The optimization problem may contain unknown parameters in its objective and constraints. The optimization problem in (3) can be reformulated as a parameterized optimization problem, according to

$$x^*(y, h) = \min_x C(x, y) \quad \text{s.t. } g(x, h) \quad (4)$$

where $y, h \in \mathfrak{X}^t$ represent parameters in the objective and constraints of the optimization problem (4). The optimization problem objective and constraints depend on these parameters. In several real-world problems, the true parameters are unknown during online solving but corresponding side information (context/feature) is available to approximate the true parameters. The context is used to train unknown parameters y_θ and h_θ to approximate y and h respectively. The training dataset to learn, say, y_θ can be represented as $\{(A^1, y_\theta^1), (A^2, y_\theta^2), \dots, (A^D, y_\theta^D)\}$, where $A^i \in \mathfrak{X}^{m \times n}$ represents contextual information matrix/feature matrix with $m \times n$ feature dimension. The feature matrix is mapped as $\mathfrak{X}^{m \times n} \rightarrow \mathfrak{X}^n$ to train n dimensional predictions y_θ (or h_θ). In ILO, the neural network (NN) parameters are trained by minimizing a regret function (L_{regret}) which is the difference between the cost of predicted decisions with the true cost and cost of optimal decisions obtained with the true cost (see (5)).

$$L_{regret} = C(x^*(y_\theta), y) - C(x^*(y), y) \quad (5)$$

The L_{regret} is minimized to find a predictor f from a class of hypothesis functions \mathcal{F} using the empirical risk minimization (ERM) principle in (6).

$$f^* = \min_{f \in \mathcal{F}} \frac{1}{D} \sum_{i=1}^D L_{regret}(y_\theta(A^i), y^i) \quad (6)$$

The ILO pipeline describing the above-mentioned procedures is shown in Fig. 1.

4.3. ILO for ED and DCOPF

The concept of ILO can be extended to train unknown parameters in the ED and DCOPF optimization models using feedback information from real power system operations. The ED optimization model have load demand ($f_{true,t}$) (demand participant load) as an unknown parameter in the power-balancing equations representing equality constraints. The DCOPF has

$f_{true,t}$ and PTDF as unknown parameters in its equality constraints. The unknown load and PTDF in the power-balancing equations are trained using ILO to minimize the cost of purchasing extra electricity by demand participants to balance supply and demand in real-time and minimize line congestion related costs.

4.3.1. Post-hoc (a posteriori) Analysis

The load and PTDF estimation using ILO to minimize extra costs on demand participants and line congestion is based on the concept of post-hoc analysis. The post-hoc analysis involves correcting decisions corresponding to forecasts using real-time true decisions.

For load training using ILO, the ED problem is initially solved using the load forecast model. Once the true load is known in real-time, the ILO minimizes an objective-specific regret function (L_{regret} (minimizing extra costs on demand participants in the current study)). The regret function is minimized by updating load forecast model parameters using gradient descent (GD) which eventually minimizes extra costs on demand participants.

For load and PTDF training, the DCOPF problem is solved using load and PTDF forecasts and corrected in real-time. The correction for DCOPF training contains two unknown parameters and thus require understanding of the impact of one parameter over the other to design the regret function as explained in the following subsection.

4.3.2. Regret Function Design for ED and DCOPF

Regret Function for ED: The L_{regret} for ED load training in this study is designed based on the concept of minimizing extra costs on consumers/demand participants due to ramping-up and -down of generators to tackle load forecast inaccuracy. The ramping-up price (bidding price (BP)) and ramping-down price (offer price (OP)) must hold the following relation with MCP

$$\begin{aligned} BP &> MCP \\ OP &< MCP \end{aligned}$$

The above-pricing relations indicate the extra price to be paid by the demand-side market participant for incorrect load estimations to the regulation market participants willing to ramp-up or -down their generation for supply-demand balancing. The regulation market players pay less when buying energy from ISO while charging more when selling energy to the ISO thereby imposing extra price/penalty to the demand participants. Inspired by the extra price/penalty concept, the L_{regret} for ILO in this work is designed as follows.

The L_{regret} (Fig. 3) for load training includes the costs corresponding to the amount of ramped-up and ramped-down powers for underestimation and overestimations in demands and their respective sub-scenarios respectively as shown in (7),

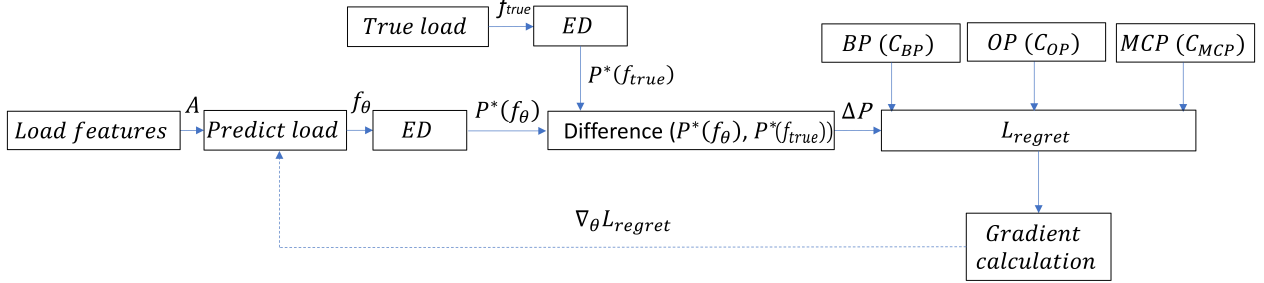


Figure 3: Load training using ILO. The predicted load (f_θ) and the true load (f_{true}) are used to solve the ED problem to generate corresponding power set-points $P^*(f_\theta)$ and $P^*(f_{true})$ respectively. The difference between the estimated and true power set-points along with the bidding price (BP), offer price (OP), and market clearing price (MCP) are used to calculate the L_{regret} using (7). The gradient to (7) is calculated using procedures described in the next sub-section and backward passed to update f_θ parameters.

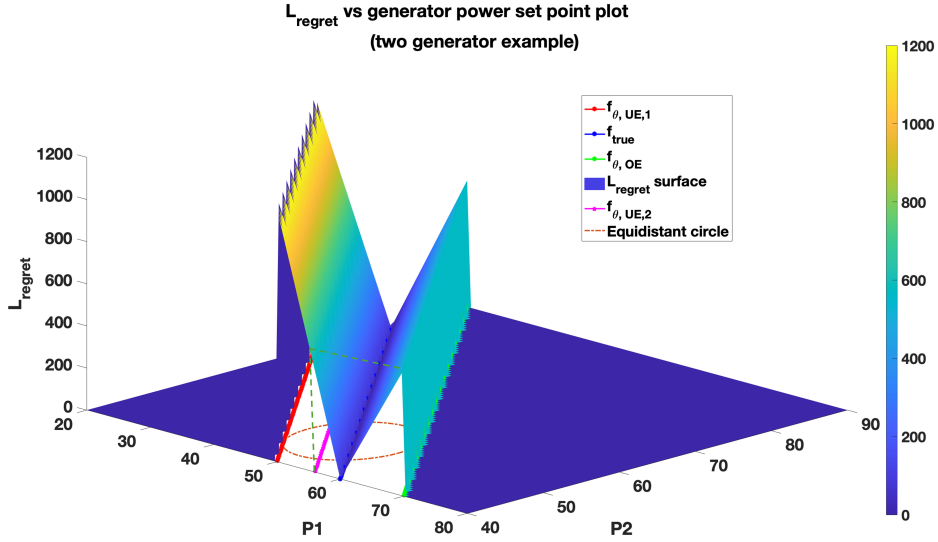


Figure 4: L_{regret} versus generator power set point ($\{P1, P2\}$) plot (two generator example). The plot represents L_{regret} surface corresponding to a load region in the x-y plane ($\{P1, P2\}$ space). The x-y plane represent feasible regions for different loads (overestimated, underestimated, and true loads). The overestimated load ($f_{\theta,OE}$) and underestimated load ($f_{\theta,UE,1}$) load are equidistant from the true load (f_{true}) represented using equidistant circle. However, as illustrated the L_{regret} corresponding to $f_{\theta,UE,1}$ is higher than the L_{regret} corresponding to $f_{\theta,OE}$. This is due to L_{regret} formulation to capture real-time market procedures of penalizing load underestimations more than overestimations. Another load underestimation within the region of interest ($f_{\theta,UE,2}$) exhibits same L_{regret} to that of $f_{\theta,OE}$; however, much closer to f_{true} compared to $f_{\theta,OE}$. The designed L_{regret} thus train the load to resemble either more overestimations or underestimations very close to the true load.

$$\begin{aligned}
L_{regret} = & \left(\sum_{i=1}^{N_G} \sum_{t=0}^{T-1} C_{BP,i,t}(S_{i,t}^-) + \sum_{i=0}^{T-1} C_{BP,ext,t}(S_{ext,t}^-) \right. \\
& + \sum_{i=1}^{N_G} \sum_{t=0}^{T-1} \left(\frac{C_{MCP,i,t}(S_{i,t}^+)}{C_{OP,i,t}(S_{i,t}^+)} \right) C_{MCP,i,t}(S_{i,t}^+) \\
& \left. + \sum_{t=0}^{T-1} \left(\frac{C_{MCP,ext,t}(S_{ext,t}^+)}{C_{OP,ext,t}(S_{ext,t}^+)} \right) C_{MCP,ext,t}(S_{ext,t}^+) \right) \\
& \text{with following constraints} \\
& S_{i,t}^+ \geq P_{i,t}^*(f_{\theta}) - P_{i,t}^*(f_{true}) \quad \forall i, t \\
& S_{i,t}^- \geq P_{i,t}^*(f_{true}) - P_{i,t}^*(f_{\theta}) \quad \forall i, t \\
& S_{ext,t}^+ \geq s_{i,t}^*(f_{\theta}) - s_{i,t}^*(f_{true}) \quad \forall i, t \\
& S_{ext,t}^- \geq s_{i,t}^*(f_{true}) - s_{i,t}^*(f_{\theta}) \quad \forall i, t \\
& S_{i,t}^+ \geq 0 \quad \forall i, t \\
& S_{i,t}^- \geq 0 \quad \forall i, t \\
& S_{ext,t}^+ \geq 0 \quad \forall i, t \\
& S_{ext,t}^- \geq 0 \quad \forall i, t
\end{aligned} \tag{7}$$

where $C_{BP,i,t}(\cdot)$, $C_{OP,i,t}(\cdot)$, $C_{MCP,i,t}(\cdot)$ and $C_{BP,ext,t}(\cdot)$, $C_{OP,ext,t}(\cdot)$, $C_{MCP,ext,t}(\cdot)$ denotes cost functions to calculate the cost of power ramping-up at BP, cost of power ramping-down at OP, cost of power production at MCP within the same region and power ramping-up at BP, cost of power ramping-down at OP, cost of power production at MCP within the different region respectively. $S_{i,t}^+$ and $S_{i,t}^-$ respectively denotes over- and under-estimation variables representing the non-negative difference between predicted and true ED decisions for generators, $S_{ext,t}^+$ and $S_{ext,t}^-$ similarly represent the non-negative differences between predicted and true ED decisions for external region. Since the cost functions in this study are assumed to be linear, the costs $C_{BP,i,t}(S_{i,t}^+)$, $C_{OP,i,t}(S_{i,t}^+)$, $C_{MCP,i,t}(S_{i,t}^+)$, $C_{BP,ext,t}(S_{i,t}^+)$, $C_{OP,ext,t}(S_{i,t}^+)$, and $C_{MCP,ext,t}(S_{i,t}^+)$ respectively are $BP_{i,t}S_{i,t}^+$, $OP_{i,t}S_{i,t}^+$, $MCP_{i,t}S_{i,t}^+$, $BP_{ext,t}S_{ext,t}^+$, $OP_{ext,t}S_{ext,t}^+$, and $MCP_{ext,t}S_{ext,t}^+$. Similar cost calculation relation holds for $S_{i,t}^-$.

The terms $\sum_{i=1}^{N_G} \sum_{t=0}^{T-1} C_{BP,i,t}(S_{i,t}^-)$ and $\sum_{t=0}^{T-1} C_{BP,ext,t}(S_{ext,t}^-)$ represents penalty on the demand participants when regulation market players selling power to ISO at higher than MCP. The terms $\sum_{i=1}^{N_G} \sum_{t=0}^{T-1} \left(\frac{C_{MCP,i,t}(S_{i,t}^+)}{C_{OP,i,t}(S_{i,t}^+)} \right) C_{MCP,i,t}(S_{i,t}^+)$ and $\sum_{t=0}^{T-1} \left(\frac{C_{MCP,ext,t}(S_{ext,t}^+)}{C_{OP,ext,t}(S_{ext,t}^+)} \right) C_{MCP,ext,t}(S_{ext,t}^+)$ represent penalty to demand participants when regulation market participants purchasing power from ISO at less than MCP.

In both cases demand participant will be penalized which in other words also means paying higher than MCP by a certain amount. The above relation thus in terms of cost due to MCP can be written as (8). The terms $\phi_{1,i,t}$ and $\phi_{ext1,t}$ represent penalty factors with respect to MCP for ramping-down, while the terms $\phi_{2,i,t}$ and $\phi_{ext2,t}$ represents the penalty factors with respect to MCP for ramping-up.

Generally, the extra price for ramping-up is higher than the amount paid for ramping-down power generation. The L_{regret} thus, in addition to minimizing the costs for incorrect load estimations is designed to penalize more load underestimations (require ramping-up) compared to load overestimations (require ramping-down) to further enhance the extra cost minimization.

The L_{regret} concept for ED is illustrated for a two generator example in Fig. 4.

$$\begin{aligned}
L_{regret} = & \left(\sum_{i=1}^{N_G} \sum_{t=0}^{T-1} \phi_{1,i,t} C_{MCP,i,t}(S_{i,t}^+) + \sum_{t=0}^{T-1} \phi_{ext1,t} C_{MCP,ext,t}(S_{ext,t}^+) \right) \\
& + \left(\sum_{i=1}^{N_G} \sum_{t=0}^{T-1} \phi_{2,i,t} C_{MCP,i,t}(S_{i,t}^-) + \sum_{t=0}^{T-1} \phi_{ext2,t} C_{MCP,ext,t}(S_{ext,t}^-) \right) \\
& \text{with following constraints} \\
& S_{i,t}^+ \geq P_{i,t}^*(f_{\theta}) - P_{i,t}^*(f_{true}) \quad \forall i, t \\
& S_{i,t}^- \geq P_{i,t}^*(f_{true}) - P_{i,t}^*(f_{\theta}) \quad \forall i, t \\
& S_{ext,t}^+ \geq s_{i,t}^*(f_{\theta}) - s_{i,t}^*(f_{true}) \quad \forall i, t \\
& S_{ext,t}^- \geq s_{i,t}^*(f_{true}) - s_{i,t}^*(f_{\theta}) \quad \forall i, t \\
& S_{i,t}^+ \geq 0 \quad \forall i, t \\
& S_{i,t}^- \geq 0 \quad \forall i, t \\
& S_{ext,t}^+ \geq 0 \quad \forall i, t \\
& S_{ext,t}^- \geq 0 \quad \forall i, t
\end{aligned} \tag{8}$$

4.3.3. Regret Function Gradient Calculation

To train the load, the L_{regret} in (7) will be minimized using the ERM principle (6) which eventually minimizes the total penalty for over- and under-estimations. The L_{regret} can be minimized using the gradient descent (GD) algorithm which requires calculating the gradient of L_{regret} in (7) with respect to unknown parameters θ . To calculate the gradient, (7) can be rewritten as:

$$\begin{aligned}
L_{regret} = & \left(\sum_{i=1}^{N_G} \sum_{t=0}^{T-1} \phi_{1,i,t} C_{MCP,i,t}(S_{i,t}^+) (\max(P_{i,t}^*(f_{\theta}) - P_{i,t}^*(f_{true}), 0)) \right. \\
& \left. + \sum_{t=0}^{T-1} \phi_{ext1,t} C_{MCP,ext,t}(S_{ext,t}^+) (\max(s_{i,t}^*(f_{\theta}) - s_{i,t}^*(f_{true}), 0)) \right) \\
& + \left(\sum_{i=1}^{N_G} \sum_{t=0}^{T-1} \phi_{2,i,t} C_{MCP,i,t}(S_{i,t}^-) (\max(P_{i,t}^*(f_{true}) - P_{i,t}^*(f_{\theta}), 0)) \right. \\
& \left. + \sum_{t=0}^{T-1} \phi_{ext2,t} C_{MCP,ext,t}(S_{ext,t}^-) (\max(s_{i,t}^*(f_{true}) - s_{i,t}^*(f_{\theta}), 0)) \right)
\end{aligned} \tag{9}$$

The differential to (9) using the total law of derivatives can be calculated as follows

$$\begin{aligned}
\nabla_{\theta} L_{regret}(f_{\theta}, f_{true}) = & \frac{\partial L_{regret}(f_{\theta}, f_{true})}{\partial \theta} \\
= & \frac{\partial L_{regret}(f_{\theta}, f_{true})}{\partial P^*(f_{\theta})} \frac{\partial P^*(f_{\theta})}{\partial f_{\theta}} \frac{\partial f_{\theta}}{\partial \theta} + \frac{\partial L_{regret}(f_{\theta}, f_{true})}{\partial s^*(f_{\theta})} \frac{\partial s^*(f_{\theta})}{\partial f_{\theta}} \frac{\partial f_{\theta}}{\partial \theta} \\
= & \left(\phi_{1,i,t} \frac{\partial C_{MCP,i,t}(S_{i,t}^+)}{\partial P^*(f_{\theta})} \frac{\partial P^*(f_{\theta})}{\partial f_{\theta}} \frac{(\max(P_{i,t}^*(f_{\theta}) - P_{i,t}^*(f_{true}), 0))}{P_{i,t}^*(f_{\theta}) - P_{i,t}^*(f_{true})} \right. \\
& \left. + \phi_{ext1,t} \frac{\partial C_{MCP,ext,t}(S_{ext,t}^+)}{\partial s^*(f_{\theta})} \frac{\partial s^*(f_{\theta})}{\partial f_{\theta}} \frac{(\max(s_{i,t}^*(f_{\theta}) - s_{i,t}^*(f_{true}), 0))}{s_{i,t}^*(f_{\theta}) - s_{i,t}^*(f_{true})} \right) \frac{\partial f_{\theta}}{\partial \theta} \\
& + \left(\phi_{2,i,t} \frac{\partial C_{MCP,i,t}(S_{i,t}^-)}{\partial P^*(f_{\theta})} \frac{\partial P^*(f_{\theta})}{\partial f_{\theta}} \frac{(\max(P_{i,t}^*(f_{true}) - P_{i,t}^*(f_{\theta}), 0))}{P_{i,t}^*(f_{true}) - P_{i,t}^*(f_{\theta})} \right. \\
& \left. + \phi_{ext2,t} \frac{\partial C_{MCP,ext,t}(S_{ext,t}^-)}{\partial s^*(f_{\theta})} \frac{\partial s^*(f_{\theta})}{\partial f_{\theta}} \frac{(\max(s_{i,t}^*(f_{true}) - s_{i,t}^*(f_{\theta}), 0))}{s_{i,t}^*(f_{true}) - s_{i,t}^*(f_{\theta})} \right) \frac{\partial f_{\theta}}{\partial \theta}
\end{aligned} \tag{10}$$

The differential terms $\frac{\partial C_{MCP,i,t}(S_{i,t}^-)}{\partial P^*(f_{\theta})}$, $\frac{\partial C_{MCP,i,t}(S_{i,t}^+)}{\partial P^*(f_{\theta})}$, $\frac{\partial C_{MCP,ext,t}(S_{ext,t}^-)}{\partial s^*(f_{\theta})}$, and $\frac{\partial C_{MCP,ext,t}(S_{ext,t}^+)}{\partial s^*(f_{\theta})}$ in (10) are straightforward to calculate and depend upon whether the cost functions $C_{MCP,i,t}$ and $C_{MCP,ext,t}$ are

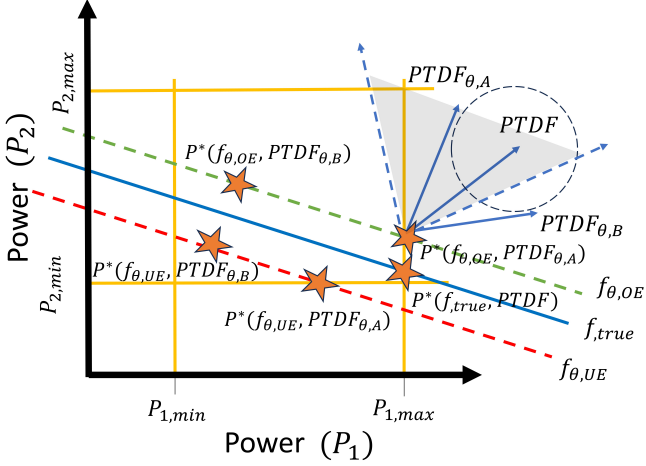


Figure 5: Feasible region for a two generator example. $f_{\theta,UE}$, $f_{\theta,true}$ and $f_{\theta,OE}$ respectively represents the predicted underestimated, true and predicted overestimated load lines. The true solution $P^*(f_{\theta,true}, PTDF)$ corresponds to true load and PTDF. The solution $P^*(f_{\theta,UE}, PTDF)$ and $P^*(f_{\theta,OE}, PTDF)$ represent optimum solutions corresponding to the under and overestimated loads ($f_{\theta,UE}$ and $f_{\theta,OE}$). The $f_{\theta,UE}$ and $f_{\theta,OE}$ cause the solution to go infeasible irrespective of the PTDF value. The $PTDF_{\theta,A}$ and $PTDF_{\theta,B}$ are two PTDF estimations. Solution corresponding to $PTDF_{\theta,A}$ ($P^*(f_{\theta,OE}, PTDF_{\theta,A})$) represents the optimum solution equal to $P^*(f_{\theta,true}, PTDF)$. The solution corresponding to $PTDF_{\theta,B}$ is the sub-optimum solution despite $PTDF_{\theta,A}$ and $PTDF_{\theta,B}$ being equidistant from the true PTDF. The gray region represents a sensitive region and any solution corresponding to PTDF forecasts within this region will be optimum. $P^*(f_{\theta,OE}, PTDF_{\theta,A})$ was estimated using ILO while $P^*(f_{\theta,OE}, PTDF_{\theta,B})$ was estimated using SLO. The similar analysis holds for $f_{\theta,UE}$ with respective solutions $P^*(f_{\theta,UE}, PTDF_{\theta,A})$ and $P^*(f_{\theta,UE}, PTDF_{\theta,B})$ corresponding to $PTDF_{\theta,A}$ and $PTDF_{\theta,B}$ respectively. For figure simplicity and clarity, the gray region is not shown for the underestimation case analysis.

linear or quadratic. In this work, as stated earlier and derived in Section 4.3.2, both the cost terms $C_{MCP,i,t}$ and $C_{MCP,ext,t}$ are linear. Similarly, the term $\frac{\partial f_{\theta}}{\partial \theta}$ in (10) is straightforward and can be evaluated using the backpropagation algorithm. The differential terms $\frac{\partial P^*(f_{\theta})}{\partial f_{\theta}}$ and $\frac{\partial S^*(f_{\theta})}{\partial f_{\theta}}$ in (10) cannot be evaluated due to discontinuity in $P^*(f_{\theta})$ resulting in gradient becoming either zero or one. An interior point (IP) based gradient calculation is used based on [27, 28] which uses logarithmic regularization to relax the discontinuous problem as explained in the next subsection.

Regret Function for DCOPF: The regret function for DCOPF is designed to train the load and the PTDF. The load training is based on the similar concept of generator ramping-up and -down. The load inaccuracy causes infeasibility in the solution, which therefore has a ramping-up/-down penalty for correction in real-time with ramping-up penalty more than the ramping-down penalty.

The PTDF matrix as well due to being in constraints causes infeasibility in the solution. The infeasibility is mainly with respect to true line flows (line flows for which DCOPF generate ED solutions). However, after thoroughly analyzing the feasible region for DCOPF, we found that the infeasibility with respect to true line flows will be mainly of four types. In one case, the infeasibility cause line flows to exceed line limits while DCOPF will give ED solution. In the second case, the line flows are violated due to infeasibility and DCOPF solution is sub-optimal with respect to ED. In the third case, the line

flows are not violated and DCOPF provide ED solutions. In the fourth case, the line flows are not violated due to infeasibility but the DCOPF solution is sub-optimal with respect to ED. In this work, we develop ILO formulations to obey the third case which will constrain line flows within line limits while approximating DCOPF solutions to ED solutions. In other words, the ILO is formulated to learn DCOPF unknown parameters to produce infeasible line flows constrained within line limits while minimizing line congestion to provide ED solutions without requiring to produce feasible line flows. PTDF is chosen as one of the learnable matrix in ILO formulation as it will achieve the aforementioned task due to its coefficients capturing system topology including line and bus configurations, and system size. Moreover, PTDF coefficients based on the system topology represents and can control power flow amounts at one line with respect to other lines. However, provided the structure of PTDF coefficients capturing various aspects of system information, the PTDF matrix cannot be directly estimated using NN as explained previously and require transformations on NN output to capture different abovementioned system information.

The PTDF estimated to produce infeasible line flows constrained within line limits and within a certain PTDF magnitude range to generate solutions approximating ED solutions will significantly minimize generator operational costs ahead of real-time and also real-time correction costs. This idea is further illustrated in a self-explanatory Fig. 5 using the feasible region of a simple two generator example. The example in Fig. 5 explains the advantage of ILO over SLO for training PTDF. Assuming the current solution to be $P^*(f_{\theta,A}, PTDF_{\theta,B})$ which is both infeasible and sub-optimal due to inaccurate load and PTDF forecasts. The correction for this solution will need correction for both infeasibility and sub-optimality. Assuming $P^*(f_{\theta,A}, PTDF_{\theta,B})$ is corrected to optimality $P^*(f_{\theta,true}, PTDF_{\theta})$, the correction/regret function will be the difference between the cost of $P^*(f_{\theta,A}, PTDF_{\theta,B})$ and $P^*(f_{\theta,true}, PTDF_{\theta})$. Moreover, since ramping-down is preferred more than ramping-up, the regret function will again be two terms with high penalty for ramping-up and low penalty for ramping-down. In addition, for a highly congested system, the line limits may get violated irrespective of the $PTDF$ value. To avoid that, the regret function will contain another term to line flows exceeding minimum or maximum line limits. Overall, the regret function will correct for infeasibility, optimality and line limit violations to train the load and the $PTDF$ forecasts,

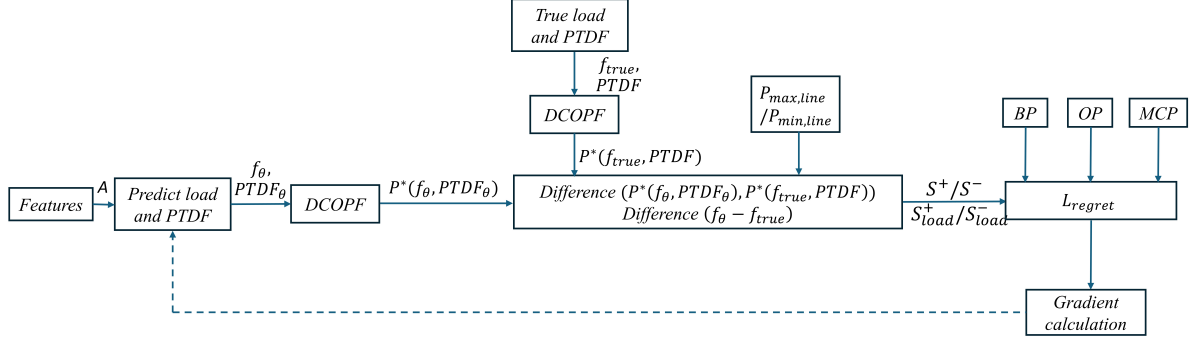


Figure 6: Load and PTDF training using ILO. The predicted load (f_θ), predicted PTDF ($PTDF_\theta$) and true load (f_{true}), true PTDF ($PTDF$) are used to solve the DCOPF problem to generate corresponding power set-points $P^*(f_\theta, PTDF_\theta)$ and $P^*(f_{true}, PTDF)$ respectively. The difference between the estimated and true power set-points along with the bidding price (BP), offer price (OP), and market clearing price (MCP) are used to calculate the L_{regret} using (11). The gradient to (11) is calculated using similar procedures as in Section 4 and backward passed to update f_θ and $PTDF_\theta$ parameters.

$$\begin{aligned}
L_{regret} = & \left(\sum_{i=1}^{N_G} \sum_{t=0}^{T-1} \phi_{1,t} C_{MCP,i,t} (S_{i,t}^+) + \sum_{t=0}^{T-1} \phi_{ext,t} C_{MCP,ext,t} (S_{ext,t}^+) \right) \\
& + \left(\sum_{i=1}^{N_G} \sum_{t=0}^{T-1} \phi_{2,t} C_{MCP,i,t} (S_{i,t}^-) + \sum_{t=0}^{T-1} \phi_{ext,t} C_{MCP,ext,t} (S_{ext,t}^-) \right) \\
& + \left(\sum_{i=1}^{N_L} \sum_{t=0}^{T-1} (S_{load,i,t}^+) \right) + \left(\sum_{i=1}^{N_L} \sum_{t=0}^{T-1} (S_{load,i,t}^-) \right) \\
& \text{with following constraints} \\
& S_{i,t}^+ \geq P_{i,t}^*(f_\theta, PTDF_\theta) - P_{i,t}^*(f_{true}, PTDF) \quad \forall i, t \\
& S_{i,t}^- \geq P_{i,t}^*(f_{true}, PTDF) - P_{i,t}^*(f_\theta, PTDF_\theta) \quad \forall i, t \\
& S_{ext,t}^+ \geq s_{i,t}^*(f_\theta, PTDF_\theta) - s_{i,t}^*(f_{true}, PTDF) \quad \forall i, t \\
& S_{ext,t}^- \geq s_{i,t}^*(f_{true}, PTDF) - s_{i,t}^*(f_\theta, PTDF_\theta) \quad \forall i, t \\
& S_{load,i,t}^+ \geq f_{\theta,OE,i,t} - f_{true,i,t} \quad \forall i, t \\
& S_{load,i,t}^- \geq f_{true,i,t} - f_{\theta,UE,i,t} \quad \forall i, t \\
& S_{i,t}^+ \geq 0 \quad \forall i, t \\
& S_{i,t}^- \geq 0 \quad \forall i, t \\
& S_{ext,t}^+ \geq 0 \quad \forall i, t \\
& S_{ext,t}^- \geq 0 \quad \forall i, t \\
& S_{load,i,t}^+ \geq 0 \quad \forall i, t \\
& S_{load,i,t}^- \geq 0 \quad \forall i, t,
\end{aligned} \tag{11}$$

where N_L denotes the number of lines. The first two terms are similar to the case 1 regret function with the difference that the correction will be for infeasibility and optimality. The last two terms are designed to penalize line flows exceeding their limits.

4.3.4. Regret Function Gradient Calculation for Case Study 2

For the case study 2 gradient calculation, again the interior point based gradient calculation technique is used. The interior point (IP) objective function for this case contain $PTDF$ matrix with dimensions of $N_L \times N_B$ where N_B denotes the number of buses. For the IEEE-14 system with 20 lines and 14 buses, the matrix size will grow very large. Moreover, the $PTDF$ coefficients in the matrix as explained previously depend upon system topology including system size, line and bus placements, and interdependency of one line over all other lines and does not follow a regular pattern that can have regular gradients. Thus, the overall gradient for the case study 2 regret function grows significantly large despite simplifications and cannot be shown in the manuscript and can be only stored as a function inside the

software. Nevertheless, the idea of IP based gradient calculations works for this case as well.

5. Results

Two different case studies were carried out. The first case study train hour and 24-hour ahead load forecasts using the ED optimization model to minimize extra costs on demand participants at each hour and for the next 24 hours respectively.

Since the load data follow a time series, with each new data point for the 24-hour case, the 24-hour ahead window shifts by one hour. The load and its features data are taken from the independent system operator New England (ISONE) website corresponding to eight load zones. The five generators in the grid have operating costs of 300, 400, 500, 600, and 700\$/MW. The maximum capacities of each generator are 2, 4, 3, 5, and 6kW.

In the second case study, the hour-ahead load and PTDFs are trained to minimize line congestion and extra costs on demand side participants. The $PTDF$ matrix coefficients are estimated by governing the NN output using transformations to capture the system topology and line impedance interdependencies. The NN output basically provide random values which are governed to capture line impedance interdependencies and system topology using certain transformations and feedback training from the captured system processes in the overall ILO pipeline. IEEE-14 bus system with six generators and eight loads is chosen in this case study. The historical data to train eight loads is obtained from eight different load zones of the independent system operator New England (ISONE) website. The features for $PTDF$ learning are the same as the load as the line congestion which is one of the objectives of this work depends on the value of load at different buses. The seven generators in the system have the operating costs of 10, 20, 30, 40, 50, 60, and 70\$/MW. The maximum capacities of each generator are 60, 70, 40, 40, 50, and 20 MW respectively.

A neural network (NN) with three layers each having 25 neurons is used for both the case studies. For both ED and DCOPF solution, the interior point optimization (IPOPT) solver [32]

was used. For model training, the pytorch and functorch libraries in python were used. In case study one, for the hour ahead case, the learning rates for ILO and SLO were set as 5×10^{-3} and the barrier coefficient (μ) was unbounded and was typically 1×10^{-9} after solving through IPOPT. For the 24-hour ahead case, the learning rates for ILO and SLO were set as 1×10^{-4} and 1×10^{-3} and the barrier coefficient (μ) was limited to 1×10^{-7} . In case study two, the learning rates for ILO were chosen as 3×10^{-4} and 4×10^{-3} respectively for load and PTDF training while for SLO load and PTDF training the learning rates were 5×10^{-3} and 2×10^{-3} respectively.

The integrated learning and optimization (ILO) training results for both case studies are compared with the sequential learning and optimization (SLO) in terms of L_{regret} value in order to compare their performance. Moreover, for case study 2, the performance of ILO for approximating sub-optimal DCOPF problem to generate ED solutions is compared with SLO by comparing their operational costs. The improved regret function and operational costs indicates significantly enhanced real-time market operations and hour-ahead generator scheduling.

5.0.1. Case Study 1: Hour Ahead and 24 Hour Ahead Load Training using ED Optimization Model

Hour Ahead Case In the hour-ahead case, the NN output is a single neuron representing the hour-ahead load prediction corresponding to the environmental features/context. The predictions trained with ILO are compared with the predictions trained with SLO to show the effectiveness of ILO in minimizing L_{regret} or maximizing the total revenue of the demand participant. Both models are trained using the load data for five days while the predictions are tested using the contextual information of the next two days. The models are trained for different over and underestimation penalty parameters (ϕ_{1i} and ϕ_{2i} respectively, $i \in$ total number of generators (N_G)) to quantify different penalty impacts on model training and L_{regret} . The penalty parameter settings are represented in Table 1. The first penalty setting corresponds to $\phi_{1i} = \phi_{2i} = 1$ which practically represents the ramp-up and ramp-down prices (BP and OP respectively) are equal to MCP. In other words, the regulation market participants will not gain profit from providing regulation services if $\phi_{1i} = \phi_{2i} = 1$. However, practically, producers/consumers willing to produce/consume extra to maintain real-time supply-demand balance would want to sell electricity at a price higher than MCP and buy electricity at less than MCP to maximize their profit. Thus, for the remaining cases, the penalty terms denote the percentage of extra money concerning MCP paid by the demand participant under study for incorrect load estimations. The value of $\phi_{2i} > \phi_{1i}$ denotes higher ramp-up costs compared to ramp-down costs. Moreover, except for the first case ($\phi_{2i} = \phi_{1i} = 1$), the ϕ_{2i} and ϕ_{1i} settings in Table 1 represent growing differences between ϕ_{2i} and ϕ_{1i} to show the impact of higher differences between ramp-up and ramp-down costs on ILO training. The training and testing results for case study 1 corresponding to all parameter settings (setting 1 - setting 5) are shown in Table 2. As observed in Table 2, the ILO trained L_{regret} exhibit smaller values than SLO for both the training and testing instances for all the settings of ϕ_{1i} and

ϕ_{2i} . Moreover, with growing differences between ramping-up and -down costs, the L_{regret} for SLO increases faster than ILO. This is due to ILO model training focusing on minimizing extra costs on the demand participant, unlike SLO which focuses on minimizing load forecast error.

24-Hour Ahead Case In the 24-hour ahead load training, the load model is trained to estimate the next 24-hour load at a one-hour time grid. The 24-hour ahead model thus forecasts 24 load values in contrast to the hour-ahead model which forecasts one load value. The training procedure for the 24-hour case is the same as for the one-hour case. The model is trained for 6 hours and tested for the next 3 hours. The training and testing L_{regret} for SLO and ILO for the 24-hour-ahead load model are shown in Table 3. The penalty parameters for the 24-hour case are set to be the same as for the one-hour case. It is observed from the results, for all the settings of penalty parameters the ILO based approach exhibit lower regret values compared to the SLO approach. The lower regret function indicates lower extra costs on the demand participants for deviation from scheduled demand.

5.0.2. Case Study 2: Hour Ahead Load and PTDF Training using DCOPF Optimization Model

In this case, the load and PTDF are trained at one hour time resolution. Provided the current feature data, the load and PTDF are predicted every next hour. The regret function is minimized using ILO to train load and PTDF. The ILO training and testing results are then compared to SLO training and testing results with the objective of minimizing the regret function. The cost vector in the regret function is chosen to be the same as the generator operating costs. This is due to the objective of congestion minimization which require expensive generators to receive higher penalties. The ramping-up and -down penalties respectively for deviations from schedule are setting1: $\phi_{1-N} = 1$, $\phi_{2-N} = 1$, setting2: $\phi_{1-N} = 1.02$, $\phi_{2-N} = 1.06$, setting3: $\phi_{1-N} = 1.05$, $\phi_{2-N} = 1.1$, setting4: $\phi_{1-N} = 1.08$, $\phi_{2-N} = 1.15$, and setting5: $\phi_{1-N} = 1.12$, $\phi_{2-N} = 1.22$, where N is the number of generators. Since, the generator operating costs are used as cost vectors assuming the pricing order of generators in RTM will remain the same as during hour-ahead scheduling, each parameter setting is equally distributed over all the generators. Table 4 illustrates the comparison between regret functions corresponding to ILO and SLO training. As observed, for all the settings of penalty parameters the regret function of ILO remains smaller than that of SLO. The smaller regret function, as explained previously, enhances economic operation by minimizing real-time correction costs and hour-ahead operational costs of generators. The ILO trains load to be either more overestimate than underestimate or train underestimate load with high accuracy while SLO trains for accuracy which may be over/underestimate and is different from ILO. For PTDF, the ILO trains the PTDFs to be within the gray region explained in Fig. 5 to obtain better optimal solutions. The decision focused training of ILO for load and PTDF minimizes the regret function.

To show the ILO capability in approximating sub-optimal DCOPF solutions to optimal ED solutions (congestion minimization) compared with SLO, the PTDF training for both ILO

Table 1: Penalty parameter settings for all grid generators (G1-G5)

Penalty parameter setting	G1		G2		G3		G4		G5	
	ϕ_{11}	ϕ_{21}	ϕ_{12}	ϕ_{22}	ϕ_{13}	ϕ_{23}	ϕ_{14}	ϕ_{24}	ϕ_{15}	ϕ_{25}
Setting 1	1	1	1	1	1	1	1	1	1	1
Setting 2	1.05	1.1	1.1	1.2	1.15	1.25	1.2	1.3	1.25	1.35
Setting 3	1.1	1.2	1.15	1.3	1.2	1.35	1.25	1.4	1.3	1.45
Setting 4	1.2	1.35	1.25	1.45	1.3	1.55	1.35	1.65	1.4	1.75
Setting 5	1.35	1.65	1.4	1.75	1.45	1.85	1.5	1.95	1.55	2.05

Table 2: Training and testing results for ILO and SLO for hour-ahead load model

Penalty parameter setting	L_{regret} ILO		Epochs ILO	L_{regret} SLO		Epochs SLO
	Training	Testing		Training	Testing	
Setting 1	0.218	0.378	100	0.428	0.646	250
Setting 2	0.224	0.288	100	0.577	0.863	250
Setting 3	0.190	0.205	100	0.591	0.854	250
Setting 4	0.180	0.230	100	0.700	1.040	250
Setting 5	0.225	0.298	100	0.814	1.130	250

Table 3: Training and testing results for ILO and SLO for 24-ahead load model

Penalty parameter setting	L_{regret} ILO		Epochs ILO	L_{regret} SLO		Epochs SLO
	Training	Testing		Training	Testing	
Setting 1	6.6	19.1	100	8.0	19.3	100
Setting 2	16.7	29.8	100	26.9	35.1	100
Setting 3	12.4	26.3	100	21.9	31.2	100
Setting 4	11.0	31.7	100	25.6	37.6	100
Setting 5	26.9	44.8	100	36.4	53.5	100

Table 4: Training and testing results for ILO and SLO for hour-ahead load and PTDF model

Penalty parameter setting	L_{regret} ILO		Epochs ILO	L_{regret} SLO		Epochs SLO
	Training	Testing		Training	Testing	
Setting 1	2015	2463	100	5188	4557	100
Setting 2	1751	2926	100	4352	3835	100
Setting 3	2375	2997	100	4775	4293	100
Setting 4	2380	2801	100	4336	4202	100
Setting 5	1310	1656	100	4846	4596	100

and SLO is compared for same load. To understand the advantage of ILO based training for congestion minimization, recall the two generator feasible region example explained in Fig. 5. The estimated PTDFs, namely $PTDF_{\theta,A}$ and $PTDF_{\theta,B}$ were equidistant from the true $PTDF$. However, $PTDF_{\theta,A}$ being ILO trained and within the sensitivity range (gray region) generate ED solution while $PTDF_{\theta,B}$ being SLO trained and outside of the sensitivity range provided sub-optimal solution. Provided that, the training results for PTDFs of ILO and SLO are illustrated in Fig. 7 to estimate their closeness to the true PTDF value which corresponds to ED solution. The plot mainly illustrates the direct 20-D NN output as 2-D using t-SNE for visualization which was guided to find correlations between line impedances given a system topology using transformations instead of plotting the transformed output. It is clearly observed, the ILO based PTDFs are far from the true value and ILO does not train for accuracy. While SLO due to accurate training is much closer to the true PTDF value.

Nevertheless, the ILO trained PTDF generate ED solutions while SLO trained PTDF despite being significantly closer to the true values generate sub-optimal solutions as explained in the following figures. Figs. 8 and 9 illustrate the hourly and total operational costs of all the generators for training and testing instances respectively obtained using ILO and SLO. The training instances are shown for 9 hours while the testing instances for 6 hours. The hourly and total operational costs of ED are used as a reference to compare with SLO.

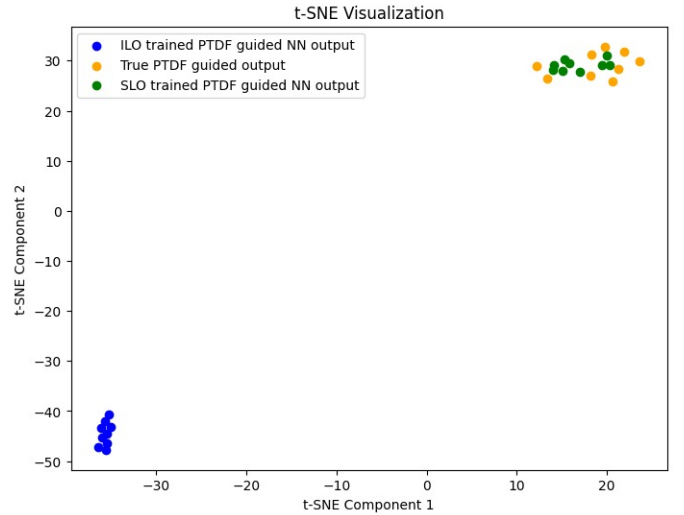


Figure 7: t-SNE analysis for PTDFs learned using ILO, and SLO with true PTDF as a reference. The plot maps the 20-D PTDF guided NN vector for each data point on the 2-D plot.

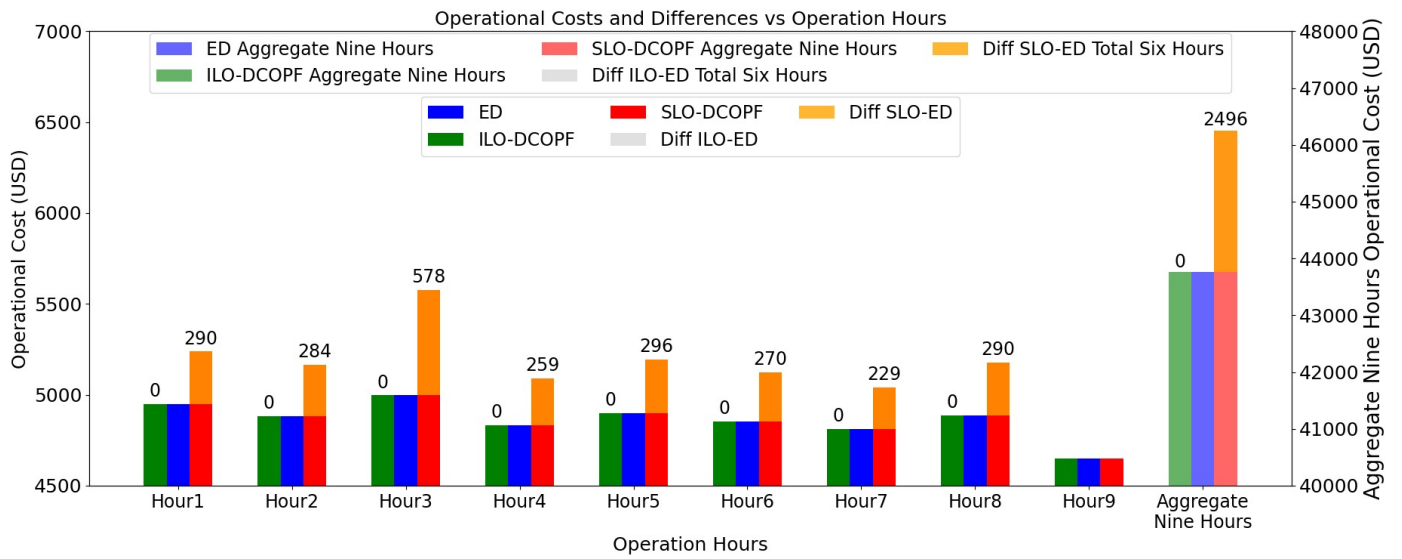


Figure 8: Hourly and total operational cost comparison between ILO and SLO for training.

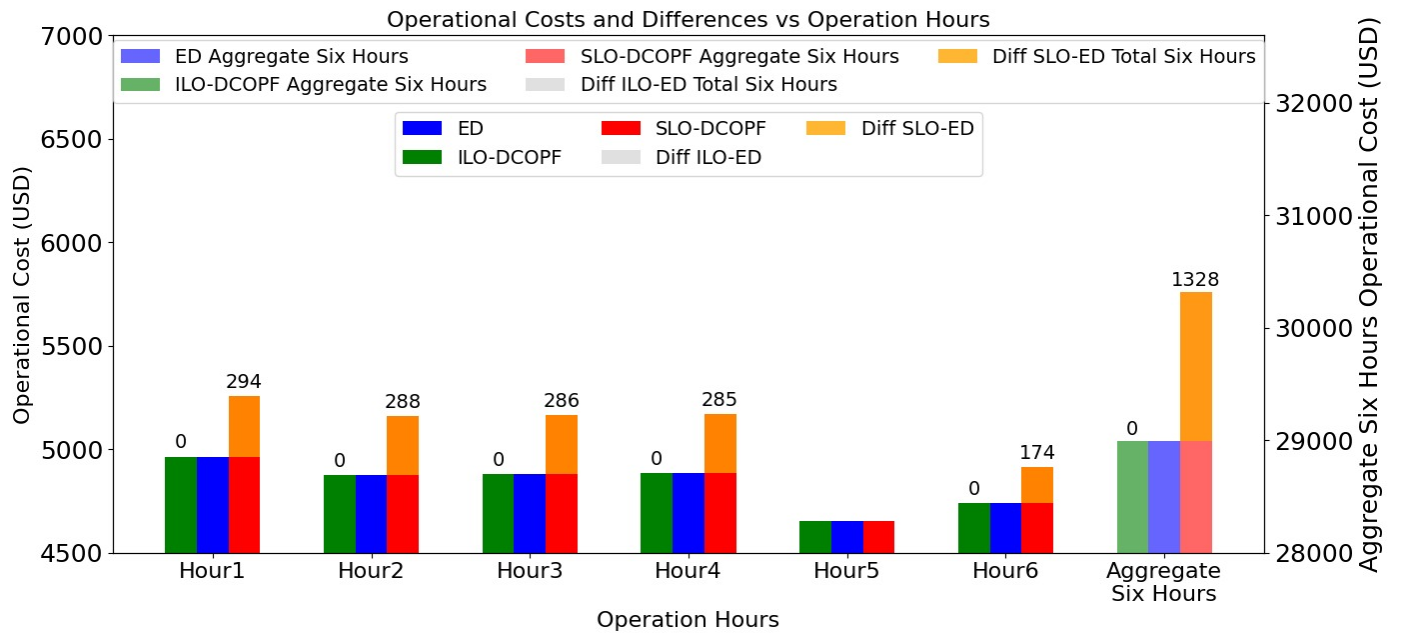


Figure 9: Hourly and total operational cost comparison between ILO and SLO for testing.

The results indicate ILO operational costs being equal to ED operational costs at all hours of operation for both training and testing instances. The trained PTFDs of ILO were much different compared to true PTFDs as shown in Fig. 7 based on t-SNE analysis while the trained PTFDs using SLO were very close to the true value; however, the ILO based DCOPF is still approximated to ED due to being within the sensitivity range as explained in Fig. 5 while SLO despite being significantly closer to true PTFDs cannot obtain true ED solutions.

6. Conclusion

As a conclusion, the proposed ILO methodologies were compared with SLO for ED and DCOPF parameter training. For both case study 1 and 2 for all the settings the ILO outperformed SLO in terms of achieving a lower regret function. The load trained using ILO for both the case studies was more an overestimate than an underestimate to achieve a lower regret function. The real-time correction costs for incorrect load and PTFD estimations were thus minimized due to better regret function training as evident in the results. Moreover, for the second case study, the lower regret function is also an indication of lower operational costs in the hour ahead scheduling as the regret function corrects for both optimality and feasibility.

References

- [1] Ye, Z.; Kim, M.K. Predicting electricity consumption in a building using an optimized back-propagation and Levenberg-Marquardt back-propagation neural network: Case study of a shopping mall in China. *Sustain. Cities Soc.* 2018, 42, 176–183.
- [2] Wang, C.; Baratchi, M.; Back, T.; Hoos, H.H.; Limmer, S.; Olhofer, M. Towards Time-Series Feature Engineering in Automated Machine Learning for Multi-Step-Ahead Forecasting. *Eng. Proc.* 2022, 18, 8017.
- [3] López-Santos, M.; Díaz-García, S.; García-Santiago, X.; Ogando-Martínez, A.; Echevarría-Camarero, F.; Blázquez-Gil, G.; Carrasco-Ortega, P. Deep Learning and transfer learning techniques applied to short-term load forecasting of data-poor buildings in local energy communities. *Energy Build.* 2023, 292, 113164.
- [4] Fan, C.; Xiao, F.; Zhao, Y. A short-term building cooling load prediction method using deep learning algorithms. *Appl. Energy* 2017, 195, 222–233.
- [5] Khan, S.; Javadi, N.; Chand, A.; Khan, A.B.M.; Rashid, F.; Afridi, I.U. Electricity Load Forecasting for Each Day of Week Using Deep CNN. *Adv. Intell. Syst. Comput.* 2019, 927, 1107–1119.
- [6] Rafi, S.H.; Al-Masood, N.; Deeba, S.R.; Hossain, E. A Short-Term Load Forecasting Method Using Integrated CNN and LSTM Network. *IEEE Access* 2021, 9, 32436–32448.
- [7] Dab, K.; Agbossou, K.; Henao, N.; Dubé, Y.; Kelouwani, S.; Hosseini, S.S. A compositional kernel based gaussian process approach to day-ahead residential load forecasting. *Energy Build.* 2022, 254, 111459.
- [8] Zeyu, W.; Yueren, W.; Rouchen, Z.; Srinivasan, R.S.; Ahrentzen, S. Random Forest based hourly building energy prediction. *Energy Build.* 2018, 171, 11–25.
- [9] Touzani, S.; Granderson, J.; Fernandes, S. Gradient boosting machine for modelling the energy consumption of commercial buildings. *Energy Build.* 2018, 158, 1533–1543.
- [10] Zhong, H.; Wang, J.; Jia, H.; Mu, Y.; Lv, S. Vector field-based support vector regression for building energy consumption prediction. *Appl. Energy* 2019, 242, 403–414.
- [11] Muhammad Bakr Abdelghany, Ahmed Al-Durra, Hatem Zeineldin, Fei Gao, Integrating scenario-based stochastic-model predictive control and load forecasting for energy management of grid-connected hybrid energy storage systems, *International Journal of Hydrogen Energy*, Volume 48, Issue 91, 2023.
- [12] Miguel A. Velasquez, Nicanor Quijano, Angela I. Cadena, Mohammad Shahidehpour, Distributed stochastic economic dispatch via model predictive control and data-driven scenario generation, *International Journal of Electrical Power & Energy Systems*, Volume 129, 2021.
- [13] Farzad Arasteh, Gholam H. Riahy, MPC-based approach for online demand side and storage system management in market based wind integrated power systems, *International Journal of Electrical Power & Energy Systems*, Volume 106, 2019.
- [14] Mostafa Yousefi Ramandi, Nooshin Bigdeli, Karim Afshar, Stochastic economic model predictive control for real-time scheduling of balance responsible parties, *International Journal of Electrical Power & Energy Systems*, Volume 118, 2020.
- [15] J. Lee et al., "Optimal Operation of an Energy Management System Using Model Predictive Control and Gaussian Process Time-Series Modeling," in *IEEE Journal of Emerging and Selected Topics in Power Electronics*, vol. 6, no. 4, pp. 1783-1795, Dec. 2018, doi: 10.1109/JESTPE.2018.2820071.
- [16] DU, Y., PEI, W., CHEN, N. et al. Real-time microgrid economic dispatch based on model predictive control strategy. *J. Mod. Power Syst. Clean Energy* 5, 787–796 (2017).
- [17] F. Garcia-Torres, C. Bordons, J. Tobajas, R. Real-Calvo, I. Santiago and S. Grieu, "Stochastic Optimization of Microgrids With Hybrid Energy Storage Systems for Grid Flexibility Services Considering Energy Forecast Uncertainties," in *IEEE Transactions on Power Systems*, vol. 36, no. 6, pp. 5537-5547, Nov. 2021, doi: 10.1109/TPWRS.2021.3071867.
- [18] M Nassourou, V Puig, J Blesa, Robust Optimization based Energy Dispatch in Smart Grids Considering Simultaneously Multiple Uncertainties: Load Demands and Energy Prices, *IFAC-PapersOnLine*, Volume 50, Issue 1, 2017.
- [19] Gan, L.K.; Zhang, P.; Lee, J.; Osborne, M.A.; Howey, D.A. Data-Driven Energy Management System With Gaussian Process Forecasting and MPC for Interconnected Microgrids. *IEEE Trans. Sustain. Energy* 2021, 12, 695–704.
- [20] Vasilj, J.; Gros, S.; Jakus, D.; Zanon, M. Day-ahead scheduling and real-time Economic MPC of CHP unit in Microgrid with Smart buildings. *IEEE Trans. Smart Grid* 2017, 10, 1992–2001.
- [21] Zhicheng Liu, Yipeng Liu, Hao Xu, Siyang Liao, Kefan Zhu, Xinxiong Jiang, Dynamic economic dispatch of power system based on DDPG algorithm, *Energy Reports*, 2022.
- [22] Ting Yang, Liyuan Zhao, Wei Li, Albert Y. Zomaya, Dynamic energy dispatch strategy for integrated energy system based on improved deep reinforcement learning, *Energy*, 2021.
- [23] Xiang Zhou, Jiye Wang, Xinying Wang, Sheng Chen, Optimal dispatch of integrated energy system based on deep reinforcement learning, *Energy Reports*, 2023.
- [24] Xinyue Wang, Haiwang Zhong, Guanglun Zhang, Guangchun Ruan, Yiliu He, Zekuan Yu, Adaptive look-ahead economic dispatch based on deep reinforcement learning, *Applied Energy*, Volume 353, Part B, 2024, 122121, ISSN 0306-2619, <https://doi.org/10.1016/j.apenergy.2023.122121>.
- [25] Bongo Y (1997) Using a financial training criterion rather than a prediction criterion. *International Journal of Neural Systems* 8(4):433–443.
- [26] Elmachtoub, Adam N. and Grigas, Paul, Smart "Predict, then Optimize", *Manage. Sci.*, 2022.
- [27] Jayanta Mandi and Tias Guns. Interior point solving for LP-based prediction+optimisation. *Advances in Neural Information Processing Systems*, 33:7272–7282, 2020.
- [28] Xinyi Hu, Jasper C.H. Lee, and Jimmy H.M. Lee., "Predict+Optimize for packing and covering LPs with unknown parameters in constraints", *Proceedings of the Thirty-Seventh AAAI Conference on Artificial Intelligence*, 2023.
- [29] Dariush Wahdany, Carlo Schmitt, Jochen L. Cremer, More than accuracy: end-to-end wind power forecasting that optimises the energy system, *Electric Power Systems Research*, Volume 221, 2023.
- [30] Wilder, Bryan, Bistra Dilkina, and Milind Tambe. "Melding the data-decisions pipeline: Decision-focused learning for combinatorial optimization." *Proceedings of the AAAI Conference on Artificial Intelligence*. Vol. 33. No. 01. 2019.
- [31] Kong, Lingkai, et al. "End-to-end stochastic optimization with energy-based model." *Advances in Neural Information Processing Systems* 35 (2022): 11341-11354.

- [32] L.T. Biegler. *Nonlinear Programming: Concepts, Algorithms and Applications to Chemical Processes*. SIAM, Philadelphia, 2010.